Research Square

Preprints are preliminary reports that have not undergone peer review.
They should not be considered conclusive, used to inform clinical practice,
or referenced by the media as validated information.

Value of Multimodal Ultrasound in Assessing Fetal Lung Maturity in Hypertensive Disorders of Pregnancy

Bin Ma
Lanzhou University Second Hospital
Ting Pan
Ultrasound Medicine Center, Gansu Provincial Maternity and Child-care Hospital
Qiong Lan
Ultrasound Medicine Center, Gansu Provincial Maternity and Child-care Hospital
Tiangang Li
Ultrasound Medicine Center, Gansu Provincial Maternity and Child-care Hospital
Zhicheng Yue
Ultrasound Medicine Center, Gansu Provincial Maternity and Child-care Hospital
Yushu He
Ultrasound Medicine Center, Gansu Provincial Maternity and Child-care Hospital
Feilei Yan
Ultrasound Medicine Center, Gansu Provincial Maternity and Child-care Hospital
Fang Nie
ery_nief@lzu.edu.cn

Lanzhou University Second Hospital

Research Article

Keywords: Hypertensive disorders of pregnancy, Ultrasound, Fetal lung maturity

Posted Date: April 15th, 2026

DOI: https://doi.org/10.21203/rs.3.rs-8989518/v1

License: This work is licensed under a Creative Commons Attribution 4.0 International License.
Read Full License

Additional Declarations: No competing interests reported.

Abstract

Objective

To investigate the value of quantitative parameters derived from multimodal ultrasound in assessing fetal lung maturity (FLM) in pregnancies complicated by hypertensive disorders of pregnancy (HDP).

Methods

This prospective study enrolled 395 women with singleton pregnancies between 24 + 0 and 40 + 6 weeks of gestation, including 130 in the HDP case group and 265 in the normal pregnancy control group. All participants underwent multimodal ultrasound examination (including two-dimensional, three-dimensional, and spectral Doppler). Quantitative measurements were obtained for fetal pulmonary structural parameters (bilateral lung areas and lung volumes) and hemodynamic parameters. Hemodynamic parameters included the peak systolic velocity to end-diastolic velocity ratio (S/D), pulsatility index (PI), and resistance index (RI) of the umbilical artery (UA) and middle cerebral artery (MCA), as well as pulmonary artery acceleration time (AT), ejection time (ET), and the AT/ET ratio. In the case group, the occurrence of neonatal respiratory distress syndrome (NRDS) was recorded. Univariate and multivariate logistic regression analyses were performed to identify independent predictors of NRDS, and a combined prediction model was constructed. The diagnostic performance of the model was evaluated using the receiver operating characteristic (ROC) curve.

Results

The incidence of NRDS in the HDP case group (31.54%) was significantly higher than that in the control group (7.92%) ($P < 0.001$). Fetuses in the case group exhibited smaller bilateral lung areas and volumes compared to the control group, with a trend of more pronounced pulmonary developmental delay as gestational age advanced. Regarding hemodynamics, the case group demonstrated a "brain-sparing effect" pattern, characterized by increased UA-PI and UA-RI alongside decreased MCA-PI and MCA-RI. Furthermore, pulmonary artery AT and the AT/ET ratio were significantly lower in the case group (all $P < 0.001$). Multivariate analysis identified gestational age (OR = 0.68), HDP (OR = 17.26), pulmonary artery AT (OR = 0.94), UA-PI (OR = 8.33), and MCA-PI (OR = 0.19) as independent predictors of NRDS. The combined prediction model yielded an area under the curve (AUC) of 0.828 (95% CI: 0.798–0.902).

Conclusion

HDP can lead to fetal pulmonary developmental delay and characteristic hemodynamic alterations. The multimodal ultrasound-based combined prediction model, incorporating gestational age, HDP status, pulmonary artery AT, UA-PI, and MCA-PI, demonstrates excellent predictive ability for the risk of NRDS.

Introduction

Hypertensive disorders of pregnancy (HDP), affecting approximately 5%–10% of pregnancies, are a leading cause of maternal and neonatal morbidity and mortality worldwide [1]. These conditions not only directly increase the risk of maternal complications such as eclampsia and placental abruption but also impair fetal lung maturity (FLM) by inducing placental dysfunction and utero-placental hypoperfusion. Studies have confirmed that neonates born to women with HDP have a significantly higher incidence of preterm birth and low birth weight, rendering them more susceptible to neonatal respiratory distress syndrome (NRDS) due to organ immaturity, which remains the leading cause of death in preterm infants [2]. Existing research has often relied on a single ultrasound modality, such as using two-dimensional ultrasound to measure lung area, three-dimensional ultrasound to assess lung volume [3, 4], or spectral Doppler alone to evaluate hemodynamics [5]. This fragmented approach fails to integrate structural and functional parameters, limiting the comprehensiveness and accuracy of FLM assessment [6]. Therefore, this study aims to integrate two-dimensional, three-dimensional, and spectral Doppler techniques to construct a multimodal ultrasound evaluation system. We will focus on analyzing the impact of HDP on fetal pulmonary structural parameters (lung area and volume) and hemodynamic parameters (UA, MCA, and pulmonary artery indices). By identifying independent predictors of NRDS and establishing a combined prediction model, we aim to provide evidence-based support for clinical FLM assessment, delivery timing decisions, and perinatal management. The ultimate goal is to reduce the incidence of NRDS and improve maternal and neonatal outcomes [7, 8].

1. Materials and Methods

1.1 Study Subjects

This prospective study was conducted in the Department of Obstetrics at Gansu Provincial Maternity and Child-care Hospital (Gansu Provincial Central Hospital) from December 2023 to December 2025. A total of 491 women with singleton pregnancies (including those with HDP and those with normal pregnancies) were initially screened. Based on strict inclusion and exclusion criteria, standard ultrasound images of fetal lungs and clinical data from 395 pregnant women between 24^{+0} and 40^{+6} weeks of gestation were ultimately included for subsequent analysis. All procedures performed in this study were in accordance with the ethical standards of the Medical Ethics Committee of Gansu Provincial Maternity and Child-Care Hospital（No.(2023) GSFY Lun Review） and with the Helsinki Declaration (as revised in 2013).

Inclusion criteria were:（Singleton pregnancy.（Gestational age between 24^{+0} and 40^{+6} weeks.（Regular antenatal check-ups and delivery at our hospital, with complete clinical history data.（Fetuses with no known congenital malformations or chromosomal abnormalities.（Pregnant women in the normal control group without other medical diseases.（Informed consent obtained and signed by the pregnant woman.

Exclusion criteria were: （Twin or multiple pregnancies.（Antenatal check-ups at our hospital but delivery elsewhere. （Fetuses with known congenital malformations or chromosomal abnormalities.（Incomplete medical history data. （Poor quality of two-dimensional, three-dimensional, or Doppler ultrasound

images.Pregnant women in the normal control group complicated by other medical diseases (thyroid disease, hypertension, heart disease, liver or kidney disease, etc.). Refusal to sign the informed consent form.

1.2 Grouping of Study Participants

A total of 395 participants were enrolled in this study, including 130 in the case group (patients with HDP) and 265 in the control group (women with normal pregnancies). To systematically analyze the influence of gestational age on fetal lung-related parameters, all participants were divided into three gestational age intervals based on the corrected gestational age (GA) on the day of ultrasound image acquisition: Group A (24^{+0} to 34^{+6} weeks), Group B (35^{+0} to 36^{+6} weeks), and Group C (37^{+0} to 40^{+6} weeks). Fetal lung ultrasound parameters were acquired and measured during the corresponding gestational windows.

1.3 Examination Equipment

This study utilized the GE Voluson E10 color Doppler ultrasound diagnostic system equipped with a CA1-7A convex array probe. During the examination, the probe depth (12–16 cm), operating frequency (2.5–7.0 MHz), total gain, and time gain compensation (TGC) were flexibly adjusted based on factors such as the maternal abdominal condition, fetal gestational age, and fetal position. This ensured uniform and clear echo signals from tissues at varying depths, thereby obtaining optimal image quality.

1.4 Examination Methods

After obtaining informed consent from the participants, basic information (name, age, gestational age), key clinical indicators (blood pressure, 24-hour urinary protein quantification), and routine obstetric ultrasound parameters were recorded in detail. Two-dimensional ultrasound, three-dimensional ultrasound, and spectral Doppler techniques were primarily employed to quantitatively measure relevant ultrasound parameters and hemodynamic indicators of the fetal lungs. All fetal ultrasound examinations were performed by physicians with at least five years of experience in ultrasound diagnosis. The selection of ultrasound images was carried out by two sonographers not involved in the subsequent analysis using a double-blind method. Fetal ultrasound examinations and fetal lung image acquisitions were performed concurrently with the routine prenatal ultrasound examinations. All images were stored in both JPG and DICOM formats.

(1) Fetal Lung Two-Dimensional Ultrasound Parameters

Fetal lung area measurement: Based on the standard fetal four-chamber view of the heart, the probe angle was finely adjusted to clearly display the atrial and ventricular structures and the atrioventricular septum, with complete inclusion of both lung fields. After obtaining the standard fetal four-chamber view, the image was frozen at end-diastole. The edges of the left and right lungs were manually traced using the trace method to obtain the left lung area and right lung area, respectively.

Fetal pulmonary artery measurement: With the pregnant woman in the supine position, a view displaying the pulmonary artery and its left and right branches was obtained. The pulmonary artery diameter was measured at the level of the pulmonary valve tips.

The AT/ET ratio measurement: The standard plane for pulmonary artery Doppler measurement was strictly defined with the angle between the probe and the fetal long axis ≤ 20°. Using a short-axis view, the pulsed Doppler sampling gate (2 mm) was placed in the mid-segment of the pulmonary artery. The angle between the ultrasound beam and the direction of blood flow was adjusted to < 20°. The blood flow waveform was displayed with a velocity scale range of 100 cm/s and a sweep speed of 200 mm/s. After clearly displaying at least five consecutive stable "biphasic" Doppler waveforms, the image was frozen. The spectrum contour was manually traced to measure acceleration time (AT) and ejection time (ET), and the AT/ET ratio was calculated. Measurements were repeated three times, and the average value was taken. All pulmonary artery velocity measurements were performed when the fetus was quiet and in the absence of uterine contractions. If contractions occurred, measurement was paused and resumed 10 minutes after the contraction ended.

(2) Fetal Lung Three-Dimensional Ultrasound Parameters

The GE Voluson E10 ultrasound system with a three-dimensional volumetric probe RM6C (depth 12–16 cm, frequency 4–8 MHz) and built-in VOCAL analysis software was used. With the fetus in a quiet state, the three-dimensional volumetric probe was selected, and the scanning angle was adjusted (45°to 85°) to acquire three-dimensional volumetric data of the fetal four-chamber view. Subsequently, using the VOCAL technique, each lung was rotated around a fixed axis (from the apex to the base of the heart) through 6 rotational planes (30°each, totaling 180°). The lung contour was manually traced on each of the 6 planes, and the software automatically reconstructed and calculated the lung volume. Each lung volume was measured three times, and the average value was taken. During the measurement process, the researcher manually reviewed and delineated the boundaries of each plane.

(3) Fetal spectral Doppler ultrasound measurement parameters

Standard measurement methods and parameters of the umbilical artery (UA): Doppler measurements of the umbilical UA should be obtained from a free-floating loop of the umbilical cord (the segment suspended in amniotic fluid), positioned as close as possible to the placental insertion site. Sampling from the intra-abdominal portion of the cord or near the fetal insertion should be avoided to minimize the influence of fetal breathing or movement on the flow velocity waveforms. After clearly visualizing the long-axis view of the umbilical cord using two-dimensional grayscale imaging, color Doppler is activated to confirm arterial blood flow (identified by its course alongside and opposite direction to the umbilical vein). The pulsed Doppler sampling gate (2–5 mm) is then placed in the center of the vessel lumen, ensuring coverage of the lumen without extending beyond the vessel wall. During measurement, the angle of insonation is maintained at ≤ 30°. Three to five consecutive, stable, and clear spectral waveforms are acquired during periods of fetal quiescence (absence of fetal movement or breathing movements). The peak systolic velocity to end-diastolic velocity ratio (S/D), pulsatility index (PI), and

resistance index (RI) are measured by manually or automatically tracing a single, complete cardiac cycle. The average value obtained from multiple measurements is used as the final result to accurately assess the resistance status of the placental-fetal circulation.

Standard measurement methods and parameters of middle cerebral artery (MCA): the standard fetal biparietal diameter view (clearly displaying the cavum septi pellucidi, thalami, and cerebral peduncles) should first be obtained. The transducer is then moved parallel towards the base of the skull to visualize the circle of Willis. The proximal segment of the MCA (approximately 1–2 cm from its origin) is selected as the sampling site, where the vessel course is relatively straight, facilitating the acquisition of stable waveforms. Gentle manipulation is required to avoid excessive transducer pressure on the fetal head, which could artificially influence intracranial hemodynamics. After activating color Doppler to identify MCA blood flow, the pulsed Doppler sampling gate (2–3 mm) is placed in the center of the vessel lumen. The angle of insonation between the ultrasound beam and the direction of blood flow is maintained at ≤ 15°–20°. Three to five consecutive stable spectral waveforms are acquired during periods of fetal quiescence, and the S/D ratio, PI , and RI are measured.

(4) Neonatal Prognosis Follow-up

The mode of delivery, sex, Apgar scores at 1 and 5 minutes after birth, and birth weight of the neonates were recorded. Fetal lung maturity was assessed, and the occurrence of neonatal respiratory distress syndrome (NRDS) was documented. The determination of fetal lung maturity required meeting all of the following criteria:Stable respiration, without signs of respiratory distress such as grunting or retractions.Chest X-ray showing good bilateral lung transparency.Blood gas analysis in room air indicating SpO2 > 90%, $PaCO_2$35–45mmHg, and no need for respiratory support. The diagnosis of NRDS met any of the following criteria: Presence of tachypnea, substernal retractions, and nasal flaring requiring continuous oxygen therapy for more than 24 hours.Administration of pulmonary surfactant therapy.Imaging findings suggestive of hyaline membrane disease. Neonates were divided into an NRDS group and a non-NRDS group based on the occurrence of NRDS. Differences in prenatal ultrasound parameters between the two groups were compared, and a prenatal prediction model for NRDS was constructed based on clinical indicators and ultrasound parameters to evaluate its predictive efficacy.

1.5 Statistical Analysis

Statistical analyses and graphical plotting were performed using SPSS software (version 26.0) and Python (version 3.8). A P-value < 0.05 was considered statistically significant. The normality of continuous variables was assessed using the Kolmogorov-Smirnov test. Variables with a normal distribution were presented as mean±standard deviation, and comparisons between groups were performed using the independent samples t-test. Non-normally distributed variables were presented as median (interquartile range), and comparisons between groups were performed using the Mann-Whitney U test. Categorical variables were expressed as frequencies (percentages), and comparisons between groups were performed using the Chi-square (χ^2) test or Fisher's exact test, as appropriate.Using the

occurrence of NRDS as the dependent variable, univariate logistic regression analysis was initially performed to screen for relevant factors. Subsequently, significant variables were included in multivariate logistic regression analysis to identify independent influencing factors for NRDS. The receiver operating characteristic (ROC) curve was plotted, and the area under the curve (AUC) was calculated to evaluate the diagnostic performance of the prediction model.

2. Results

2.1 Clinical Baseline Characteristics

No statistically significant differences were observed between the two groups in terms of maternal age ($P = 0.079$) and neonatal sex distribution ($P = 0.214$). Regarding gestational age distribution, the proportion of early-to-mid preterm pregnancies in the case group was significantly higher than that in the control group (49.23% vs. 13.21%), whereas the proportion of term pregnancies was significantly lower (13.85% vs. 43.02%) ($P < 0.001$). In terms of delivery mode, the Cesarean section rate was significantly higher in the case group compared to the control group (68.46% vs. 12.08%) ($P < 0.001$). Concerning neonatal outcomes, the case group exhibited significantly lower birth weight (2700.50 g vs. 3110.00 g, $P < 0.001$) and a significantly higher proportion of neonates with Apgar scores ≤ 7 (30.00% vs. 12.45%, $P < 0.001$). Furthermore, the incidence of NRDS was significantly higher in the case group than in the control group (31.54% vs. 7.92%, $P < 0.001$). These results indicate significant differences between the case and control groups regarding gestational age distribution, mode of delivery, neonatal birth weight, Apgar scores, and NRDS incidence (See Table 1).

2.2 Characteristic Analysis of Fetal Multimodal Ultrasound Parameters

Comparison of multimodal ultrasound parameters between the two groups revealed that the case group exhibited significantly smaller pulmonary structural and volumetric indices (left and right lung areas and volumes) compared to the control group (all $P < 0.001$), suggesting potential restriction in pulmonary development (See Fig. 1, 2, 3). No significant difference was observed in pulmonary artery diameter between the two groups ($P = 0.267$); however, the case group demonstrated significantly lower acceleration time (AT) and AT/ejection time (ET) ratio (both $P < 0.001$), reflecting abnormal pulmonary artery hemodynamics (See Figures 4, 5). Furthermore, umbilical artery (UA) Doppler parameters (S/D, PI, RI) were significantly elevated in the case group (all $P < 0.001$), indicating increased placental resistance. In contrast, middle cerebral artery (MCA) parameters (S/D, PI, RI, PSV) were significantly decreased (all $P < 0.001$), consistent with the "brain-sparing effect" observed in response to fetal hypoxia (See Table 2).

2.3 Gestational Age-Related Differences in Fetal Multimodal Ultrasound Parameters

Analysis of gestational age-related differences in multimodal ultrasound parameters within the control group revealed that, with the exception of ET ($P = 0.799$), all other parameters differed significantly among the three gestational age groups ($P < 0.001$). As gestational age advanced, pulmonary developmental parameters (left and right lung areas and volumes) increased progressively, the

pulmonary artery diameter widened, AT prolonged, and the AT/ET ratio increased. Concurrently, UA and MCA parameters (S/D, PI, RI) demonstrated a decreasing trend, while MCA-PSV peaked in the mid-gestation group (60.0 ± 8.0 cm/s). These findings indicate that in normal pregnancy, fetal pulmonary development, cardiac function, and hemodynamic parameters exhibit regular changes with advancing gestational age (See Table 3).

Analysis of gestational age-related differences in multimodal ultrasound parameters within the case group revealed that pulmonary development-related indicators, including left and right lung areas and volumes, differed significantly among the three groups ($P < 0.001$), with lung areas showing an increasing trend as gestational age advanced. Pulmonary artery diameter, AT, and the AT/ET ratio increased significantly with advancing gestation ($P < 0.001$), whereas ET showed no significant change ($P = 0.799$). Regarding UA and MCA parameters, S/D, PI, and RI all demonstrated a decreasing trend with increasing gestational age ($P < 0.001$), indicating a gradual reduction in placental and cerebral vascular resistance. MCA-PSV was highest in Group B (50.0 ± 5.25 cm/s), with significant differences observed among the groups ($P < 0.001$) (See Table 4).

2.4 Construction of an NRDS Prediction Model Based on Multimodal Ultrasound

No statistically significant difference was observed in maternal age between the NRDS group and the non-NRDS group ($P > 0.05$). However, a highly significant difference was found in the distribution of gestational age between the two groups ($P < 0.001$). Specifically, in the NRDS group, the highest proportion of neonates (49.23%) were born prematurely between 24+0 and 34+6 weeks of gestation. In contrast, in the non-NRDS group, the highest proportion (43.02%) were full-term neonates born between 37+0 and 40+6 weeks of gestation. Furthermore, the incidence of HDP was significantly higher in the NRDS group (31.54%) compared to the non-NRDS group (7.92%), with the difference being statistically significant ($P < 0.001$). Regarding pulmonary structural parameters, left and right lung areas, as well as left and right lung volumes, were significantly smaller in the NRDS group than in the non-NRDS group (all $P < 0.001$). Concerning functional parameters, the AT and AT/ET ratio were significantly lower in the NRDS group compared to the non-NRDS group ($P < 0.001$). No significant differences were observed between the two groups in pulmonary artery diameter ($P = 0.267$) or ET ($P = 0.199$). In terms of UA hemodynamic parameters, S/D, PI, and RI were all significantly higher in the NRDS group than in the non-NRDS group ($P < 0.001$). For MCA hemodynamic parameters, S/D, PI, and PSV were significantly lower in the NRDS group compared to the non-NRDS group ($P < 0.001$). Notably, the MCA-RI was also significantly reduced in the NRDS group ($P < 0.001$) (See Table 5).

Regarding clinical baseline characteristics, an increase in gestational age significantly reduced the risk of NRDS (OR = 0.64, 95% CI: 0.55–0.75, $P < 0.001$), whereas HDP emerged as an extremely strong risk factor for NRDS (OR = 42.92, 95% CI: 13.78–133.70, $P < 0.001$). Analysis of pulmonary structural parameters revealed that all measured indicators were significant protective factors: left lung area (OR = 0.79, 95% CI: 0.71–0.87), right lung area (OR = 0.76, 95% CI: 0.69–0.83), left lung volume (OR = 0.81, 95% CI: 0.75–0.88), and right lung volume (OR = 0.80, 95% CI: 0.74–0.87), all with $P < 0.001$. Among

pulmonary functional parameters, AT and the AT/ET ratio were negatively associated with the risk of NRDS (OR = 0.92, 95% CI: 0.89–0.96; OR = 0.56, 95% CI: 0.44–0.71, respectively), and both associations were statistically significant ($P < 0.001$). Umbilical artery hemodynamic parameters exhibited a characteristic distribution: PI and RI were both strong risk factors (OR = 17.30, 95% CI: 6.24–47.94; OR = 17.36, 95% CI: 6.38–47.20, respectively). In contrast, corresponding MCA parameters acted as protective factors, with the protective effect of RI being particularly pronounced (OR = 0.01, 95% CI: 0.00–0.09, $P < 0.001$) (See Table 6).

Based on the results of univariate logistic regression analysis and clinical expertise, variables were selected for inclusion in the multivariate model. All selected variables demonstrated highly significant statistical significance in the univariate analysis ($P < 0.001$), and their odds ratios (OR) indicated substantial clinical effect sizes, particularly for HDP (OR = 42.92) and UA-PI (OR = 17.30), suggesting their substantial impact on NRDS risk. This selection was guided by the following multidimensional considerations. First, HDP serves as an upstream etiological initiating factor, closely linked to NRDS occurrence through its effects on the fetal-placental circulation. Gestational age represents a fundamental temporal measure of fetal lung maturity, while pulmonary artery AT reflects right ventricular function and pulmonary vascular resistance. Second, considering the clinical interrelationships among variables and potential multicollinearity, we prioritized indicators with clear pathophysiological significance and strong representativeness. For instance, among UA parameters, PI was preferentially selected over RI or S/D, as it is considered to more stably reflect downstream placental resistance. Regarding MCA parameters, although RI exhibited a seemingly more extreme OR value (OR = 0.01), we opted for PI (OR = 0.15) because PI precisely indicates the compensatory cerebral blood flow redistribution triggered by fetal hypoxia and is more widely accepted in academic research as an indicator for assessing cerebral hemodynamics. Ultimately, these five indicators comprehensively encompass multiple key pathophysiological aspects of NRDS pathogenesis, collectively forming an evaluation system that covers maternal factors, fetal developmental status, placental function, and fetal hemodynamic characteristics, enabling a comprehensive assessment of NRDS risk.

Based on the results of multivariate logistic regression analysis, five independent predictors of NRDS were identified in this study. Gestational age (OR = 0.68, 95% CI: 0.57–0.81, $P < 0.001$), AT (OR = 0.94, 95% CI: 0.90–0.98, $P = 0.003$), and MCA-PI (OR = 0.19, 95% CI: 0.05–0.72, $P = 0.015$) were identified as independent protective factors against NRDS. Conversely, HDP (OR = 17.26, 95% CI: 5.12–58.21, $P < 0.001$) and UA-PI (OR = 8.33, 95% CI: 2.67–25.97, $P < 0.001$) emerged as independent risk factors. These results indicate that after controlling for other confounding variables, gestational age, HDP, UA and MCA hemodynamic parameters, and pulmonary artery AT—reflecting right ventricular function—possess independent predictive value for the occurrence of NRDS (See Table 7).

Compared with single predictors such as HDP, gestational age, UA-PI, MCA-PI, or AT, the NRDS prediction model constructed from the five independent predictors yielded an AUC of 0.828 (95% CI: 0.798–0.902), with accuracy, sensitivity, and specificity of 75.2%, 80.1%, and 74.3%, respectively, demonstrating significantly superior diagnostic performance compared with any single indicator alone. The AUC values

for each of the aforementioned independent predictors were as follows: HDP 0.718, gestational age 0.752, UA-PI 0.795, MCA-PI 0.683, and AT 0.724, all of which were significantly lower than that of the combined prediction model (See Table 8). This combined model, which integrates clinical baseline characteristics, UA and MCA hemodynamic parameters, and pulmonary functional parameters, exhibits good predictive ability for the risk of NRDS occurrence (See Fig. 6).

3. Discussion

Hypertensive disorders of pregnancy (HDP), a common and severe complication in obstetrics, are pathologically rooted in shallow placental implantation, inadequate spiral artery remodeling, and systemic vascular endothelial dysfunction. This series of pathological changes not only directly underlies maternal clinical symptoms such as hypertension and proteinuria but also leads to placental hypoperfusion and significant oxidative stress, exerting a sustained negative impact on the developmental processes of multiple fetal organ systems [9, 10]. The results of the present study demonstrate that the proportions of low birth weight neonates, low Apgar scores (≤ 7), and the incidence of NRDS were significantly higher in the HDP case group compared to the control group. Notably, the case group exhibited a markedly high Cesarean section rate of 68.46%, primarily attributable to acute deterioration of HDP (e.g., progression to severe preeclampsia with serious complications) or fetal distress, circumstances compelling clinicians to intervene urgently by terminating the pregnancy. It is important to recognize that, compared with vaginal delivery, Cesarean section without the compressive effect of the birth canal is itself an independent risk factor for transient tachypnea of the newborn and wet lung. Therefore, the observed increase in adverse neonatal respiratory outcomes (including NRDS) in the case group is associated with this mode of delivery in a manner that cannot be overlooked. These findings corroborate the conclusions of Gagliardi et al. [11], further establishing HDP as an independent risk factor for delayed fetal lung development and profoundly reflecting the significant perinatal clinical challenges faced by women with HDP and their neonates.

Following the establishment of the overall impact of HDP on neonatal outcomes, this study further employed dynamic fetal pulmonary developmental parameters to delve into the specific influence pattern of HDP on the trajectory of fetal lung development. The results demonstrated that although left and right lung areas and volumes in both the case and control groups exhibited the expected continuous increasing trend with advancing gestational age, the measured values of all pulmonary developmental indicators in the case group were systematically lower than those in the control group throughout the entire observation period. Crucially, the disparity between the two groups progressively widened as gestation advanced. Fetal lung development enters a critical "accelerated growth phase" after 28 weeks of gestation, characterized by a rapid doubling of alveolar number and significant maturation of the pulmonary microvascular network, with peak demands for energy and oxygen supply [12]. However, under the pathological state of HDP, the already dysfunctional placenta struggles to adequately meet the additional metabolic demands of lung development during this phase, resulting in a relative lag in fetal pulmonary growth velocity in the case group. The further slowing of lung volume growth observed after 34 weeks of gestation directly reflects this pathological process. This finding is highly consistent with

the conclusions of Sabogal et al. [13], collectively validating the significant value of ultrasound imaging in the early identification of HDP-related delayed fetal lung development. This suggests that the impact of HDP on fetal lung development is not a static event confined to a specific gestational week, but rather a dynamic, progressive process beginning in the second trimester and extending into the third, with its inhibitory effect being most pronounced during the most critical late phase of lung development [14].

Delayed pulmonary structural development is closely associated with adaptive hemodynamic remodeling occurring in fetuses under the pathological condition of HDP, with both factors collectively constituting the pathophysiological framework influencing fetal lung maturity (FLM). Placental insufficiency resulting from HDP serves as the initiating factor for adverse maternal and fetal outcomes. On one hand, it directly inhibits the proliferation and differentiation of fetal lung parenchymal cells; on the other hand, by triggering the "brain-sparing effect" and increasing pulmonary circulation resistance, it further restricts lung growth and functional maturation from the perspective of blood perfusion [15]. The Doppler parameters obtained in this study provide direct evidence for this mechanism: UA-S/D, PI, and RI values were significantly elevated in the case group, reflecting increased placental vascular resistance. Concurrently, MCA-S/D, PI, and RI values were significantly reduced, a direct consequence of fetal cardiac output redistribution—prioritizing blood flow to vital organs such as the brain and heart while reducing perfusion to non-vital organs like the lungs and kidneys. Although this compensatory mechanism helps maintain the stability of fetal vital centers in the short term, prolonged pulmonary hypoperfusion can disrupt the normal development and architecture of the pulmonary vascular bed, potentially impairing the synthesis of pulmonary surfactant by alveolar type II cells, ultimately exerting a profound negative impact on FLM. This pattern of hemodynamic alteration is entirely consistent with the classic description by Wolf et al [16]. Furthermore, Doppler analysis of the pulmonary artery revealed significantly lower AT and AT/ET ratio in fetuses from the case group compared to the control group ($P < 0.001$), aligning with the observations of Dayanan et al [5]. A deeper hemodynamic analysis indicates that AT reflects the acceleration of pulmonary artery blood flow; its shortening directly suggests increased pulmonary vascular resistance. The reduced AT/ET ratio indicates a relatively prolonged period during right ventricular ejection when the ventricle faces high resistance, serving as a functional indicator of pulmonary vascular bed dysplasia. These abnormal parameter changes are closely related to pulmonary vasoconstriction triggered by chronic fetal hypoxia and acidosis resulting from HDP. Compared with the study by Tang et al [17], the innovation of this research lies in systematically delineating the characteristic alterations of these parameters specifically within the HDP population and establishing their association with delayed lung development, thereby providing a more specific theoretical basis for clinically utilizing non-invasive Doppler techniques to assess pulmonary circulation status. The potential underlying physiological mechanisms may involve pulmonary vasoconstriction induced by chronic hypoxia and acidosis, as well as secondary pulmonary vascular bed dysplasi.

Beyond systematically analyzing the impact of HDP on fetal pulmonary structure and hemodynamics, integrating all key indicators to construct a precise predictive model for NRDS represents the final step in translating this research toward clinical application. This study confirmed that the incidence of NRDS in neonates born to women with HDP was 31.54%, significantly higher than the 7.92% observed in the

control group. This finding robustly reinforces, from a clinical outcome perspective, that HDP is an independent risk factor for delayed fetal lung development. An integrated analysis from a pathophysiological perspective reveals that placental insufficiency resulting from HDP initially leads to placental hypoperfusion, subjecting the fetus to a chronic hypoxic environment. This, in turn, activates the fetal renin-angiotensin system, triggering pulmonary vasoconstriction and increasing pulmonary vascular resistance, thereby creating a vicious cycle of "hypoxia-vasoconstriction-reduced perfusion" that directly impairs normal lung development. Secondly, the chronic hypoxic state specifically inhibits the function of alveolar type II cells, reducing the synthesis and secretion of pulmonary surfactant [12]. These substances are crucial for maintaining alveolar stability; their deficiency predisposes alveoli to collapse at end-expiration, which constitutes the fundamental pathological basis for NRDS. A prospective study by Rios et al [18] previously indicated that the AT/ET ratio exhibits superior sensitivity in predicting NRDS compared to traditional two-dimensional ultrasound parameters. Building upon this foundation, the present study further advanced the field by constructing a comprehensive NRDS predictive model using multivariate logistic regression analysis. This model identified gestational age, HDP, UA-PI, MCA-PI, and pulmonary artery AT as independent predictors of NRDS. Among these, gestational age, MCA-PI, and AT were identified as protective factors, whereas HDP and UA-PI were risk factors. These indicators not only cover multiple key pathophysiological links in the pathogenesis of NRDS but also collectively constitute a comprehensive evaluation system encompassing maternal underlying disease, fetal developmental maturity, placental function, and fetal hemodynamic compensatory status. Ultimately, the combined prediction model constructed from these five independent predictors exhibited excellent diagnostic efficacy, with an AUC as high as 0.828, demonstrating significantly superior diagnostic performance compared to any single predictor alone. This result confirms the distinct advantage of multi-parameter combined assessment in predicting NRDS, with its efficacy surpassing that of the single-parameter predictive models reported by Palacio et al.

In summary, this study, utilizing a multimodal ultrasound system, has systematically elucidated the impact pathway of HDP on fetal lung development and, based on these findings, established a clinically promising predictive model for NRDS risk. However, it is essential to objectively acknowledge the limitations of the current research. First, this study employed a single-center retrospective design. Although the sample size met basic statistical requirements, the inclusion of only 130 HDP cases may have limited the power for subgroup analyses, and single-center data are inevitably subject to selection bias. Therefore, the generalizability of the study conclusions requires further validation through multicenter, large-sample prospective studies. Second, while the combined prediction model demonstrated good diagnostic efficacy, the parameters included in the model were primarily derived from ultrasound measurements obtained during the mid-to-late third trimester (≥ 28 weeks). Longitudinal tracking analysis of the dynamic evolution of HDP's impact on fetal lung development during earlier stages (e.g., 20–24 weeks) was not performed. Future studies could be designed with serial observations at multiple time points to elucidate the complete time window and critical junctures of HDP's influence on lung development. Third, regarding the assessment of pulmonary hemodynamics,

this study primarily employed Doppler spectral parameters such as AT and AT/ET, but did not incorporate newer ultrasound technologies, such as superb microvascular imaging or three-dimensional power Doppler quantitative analysis. These techniques may offer greater sensitivity in evaluating pulmonary microcirculatory perfusion status. Fourth, although multivariate regression analysis was used to adjust for certain confounding factors, the potential influence of unmeasured confounding variables (e.g., maternal nutritional status, completion of antenatal corticosteroid course, differences in specific medication regimens) on the study results cannot be excluded. Finally, fetal lung functional maturation is a complex process involving both structural development and biochemical maturation. This study primarily relied on morphological and hemodynamic indicators for indirect assessment. Future research endeavors that integrate the detection of biochemical markers related to pulmonary surfactant in amniotic fluid or fetal tracheal aspirate, or that combine macroscopic imaging indicators with microscopic molecular markers, hold promise for constructing a more comprehensive FLM evaluation system.

4. Conclusion

This study, by integrating two-dimensional, three-dimensional, and spectral Doppler ultrasound techniques, established a multimodal evaluation system. It systematically revealed the characteristics of progressive fetal lung developmental delay associated with HDP as gestational age advances, and identified a concomitant hemodynamic compensatory pattern characterized by increased UA resistance, decreased MCA resistance, and a reduced pulmonary artery AT/ET ratio. Based on multivariate analysis, five independent predictors—gestational age, HDP, pulmonary artery AT, UA-PI, and MCA-PI—were identified, and a predictive model for NRDS with excellent performance was constructed. This study provides a new perspective for understanding the pathophysiological mechanisms of fetal lung development in the context of HDP and offers an effective tool for the precise clinical prediction of NRDS risk.

Abbreviations

HDP	Hypertensive Disorders of Pregnancy
FLM	Fetal Lung Maturity
NRDS	Neonatal Respiratory Distress Syndrome
AT	Acceleration Time
ET	Ejection Time
UA	Umbilical Artery
MCA	Middle Cerebral Artery
S/D	Peak Systolic Velocity / End-Diastolic Velocity Ratio
PI	Pulsatility Index
RI	Resistance Index
PSV	Peak Systolic Velocity
ROC	Receiver Operating Characteristic
OR	Odds Ratio
AUC	Area Under the Curve
CI	Confidence Interval
GA	Gestational Age
TGC	Time Gain Compensation
VOCAL	Virtual Organ Computer-aided Analysis
ACC	Accuracy
SEN	Sensitivity
SPE	Specificity

Declarations

Acknowledgments

The authors would like to express their gratitude to the patients and their families who participated in this study.We would also like to thank the medical and research staff at Gansu Maternal and Child Health Hospital for their support and assistance in conducting this research.

Author contributions

(I) Conception and design: B Ma, T Pan, Q Lan; (II) Administrative support: F Nie; (III) Provision of study materials or patients: B Ma, T Li ; (IV) Collection and assembly of data: B Ma, T Pan, Z Yue, Y H; (V) Data analysis and interpretation: T Pan, Q Lan, F Yan; (VI) Manuscript writing: All authors; (VII) Final approval of manuscript: All authors.

Funding

This work was supported by the Science and Technology Program of Gansu Province (Grant No. 23JRRA1383).

Data availability

The article includes a list (Tables) of all cases presenting data used to support this study's findings.

Ethics approval and consent to participate

This study has been approved by the Medical Ethics Committee of Gansu Provincial Maternity and Child-Care Hospital (Approval No.: [2023] GSFY Ethics Review [65]). All procedures performed in this study strictly followed the ethical standards of this committee and the provisions of the Declaration of Helsinki (revised in 2013).

Consent for publication

The clinical data and imaging materials used in this study were obtained with written informed consent from the legal guardians of the study participants, with the scope of authorization encompassing their use for scientific research and academic publication. All relevant materials will be made publicly available in accordance with the applicable intellectual property sharing license agreement.

Competing interests

The authors declare no competing interests.

Author details

[1]Ultrasound Medicine Center, Lanzhou University Second Hospital, Lanzhou, Gansu Province, China,730050

[2]Ultrasound Medicine Center, Gansu Provincial Maternity and Child-care Hospital, Lanzhou, Gansu Province,China,730050

Clinical trial number: not applicable.

References

1. STEYERBERG E W, VICKERS A J, COOK N R, et al. Assessing the performance of prediction models: a framework for traditional and novel measures [J]. Epidemiology, 2010, 21(1): 128-138.
2. JIANG Y, YANG M, WANG S, et al. Emerging role of deep learning-based artificial intelligence in tumor pathology [J]. Cancer Commun (Lond), 2020, 40(4): 154-166.
3. LEE A, PARK G C, CHO E S, et al. Radiomics-based sialadenitis staging in contrast-enhanced computed tomography and ultrasonography: a preliminary rat model study [J]. Oral Surg Oral Med Oral Pathol Oral Radiol, 2023, 136(2): 231-239.
4. SUN H, JIAO J, WANG Y, et al. Ultrasound based radiomics model for assessment of placental function in pregnancies with preeclampsia [J]. Sci Rep, 2024, 14(1): 21123.
5. VICKERS A J, ELKIN E B. Decision curve analysis: a novel method for evaluating prediction models [J]. Med Decis Making, 2006, 26(6): 565-574.
6. HAN T, JIN X D, YANG J F, et al. Clinical Analysis of Fetal Lung Development Index and Pregnancy Outcome in Pregnant Women with Gestational Diabetes Mellitus with Satisfactory Blood Glucose Control [J]. Contrast Media Mol Imaging, 2022, 2022: 5777804.
7. PARRA-SAAVEDRA M, CROVETTO F, TRIUNFO S, et al. Placental findings in late-onset SGA births without Doppler signs of placental insufficiency [J]. Placenta, 2013, 34(12): 1136-1141.
8. ABMAN S H. Bronchopulmonary dysplasia: "a vascular hypothesis" [J]. Am J Respir Crit Care Med, 2001, 164(10 Pt 1): 1755-1756.
9. WANG J, CHEN Z, ZHANG H, et al. A machine learning model based on placental magnetic resonance imaging and clinical factors to predict fetal growth restriction [J]. BMC Pregnancy Childbirth, 2025, 25(1): 325.
10. SERIZAWA M, MAEDA K. Noninvasive fetal lung maturity prediction based on ultrasonic gray level histogram width [J]. Ultrasound Med Biol, 2010, 36(12): 1998-2003.
11. MOETY G A, GAAFAR H M, EL RIFAI N M. Can fetal pulmonary artery Doppler indices predict neonatal respiratory distress syndrome? [J]. J Perinatol, 2015, 35(12): 1015-1019.
12. Lizhen Z, Linfeng Y, Ren M, et al. Relationship between normal fetal pulmonary artery Doppler parameters and gestational age. Chin J Med Ultrasound (Electron Ed). 2019;16(11):848-852.
13. SYED A B, ZOGA A C. Artificial Intelligence in Radiology: Current Technology and Future Directions [J]. Semin Musculoskelet Radiol, 2018, 22(5): 540-545.
14. RUANO R, TAKASHI E, DA SILVA M M, et al. Prediction and probability of neonatal outcome in isolated congenital diaphragmatic hernia using multiple ultrasound parameters [J]. Ultrasound Obstet Gynecol, 2012, 39(1): 42-49.
15. RUANO R, MARTINOVIC J, DOMMERGUES M, et al. Accuracy of fetal lung volume assessed by three-dimensional sonography [J]. Ultrasound Obstet Gynecol, 2005, 26(7): 725-730.
16. LABAN M, MANSOUR G M, EL-KOTB A, et al. Combined measurement of fetal lung volume and pulmonary artery resistance index is more accurate for prediction of neonatal respiratory distress syndrome in preterm fetuses: a pilot study [J]. J Matern Fetal Neonatal Med, 2019, 32(4): 626-632.

17. Yong G, Xiaoyan H, Jianfeng S, et al. Accuracy of Three-Dimensional Ultrasound VOCAL Technique in Measuring Fetal Lung Volume in Fetuses with Congenital Heart Disease. Chin J Ultrasound Med. 2019;35(06):531-534.
18. LITJENS G, KOOI T, BEJNORDI B E, et al. A survey on deep learning in medical image analysis [J]. Med Image Anal, 2017, 42: 60-88.

Tables

Tables 1 to 8 are available in the Supplementary Files section.

Figures

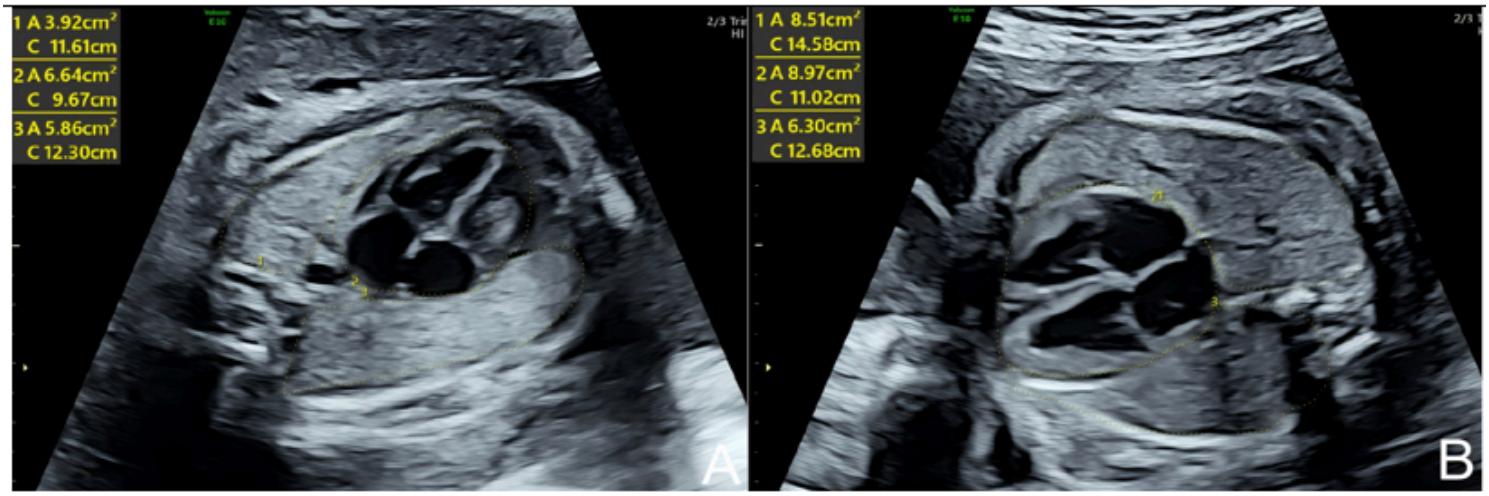


Figure 1

Application of the trace method to delineate the borders of the left and right lungs for measuring lung areas in a fetus at 30 weeks of gestation (A-B): (A) In the case group, the left lung area was 3.92 cm², and the right lung area was 5.86 cm²; (B) In the control group, the left lung area was 6.30 cm², and the right lung area was 8.51 cm².(cm²: square centimeters)

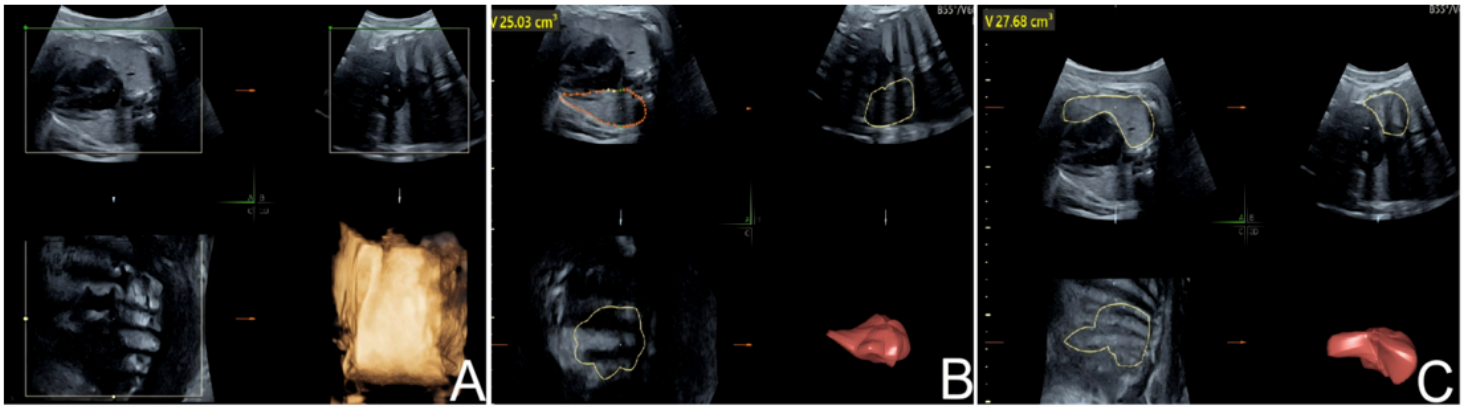


Figure 2

Application of three-dimensional VOCAL technique for measuring fetal lung volume at 34 weeks of gestation in the case group (A-C): (A) Three-dimensional view of the fetal four-chamber transverse view; (B) Left lung volume measured 25.03 cm³; (C) Right lung volume measured 27.68 cm³.(VOCAL:Virtual Organ Computer-aided Analysis; cm³: cubic centimeters)

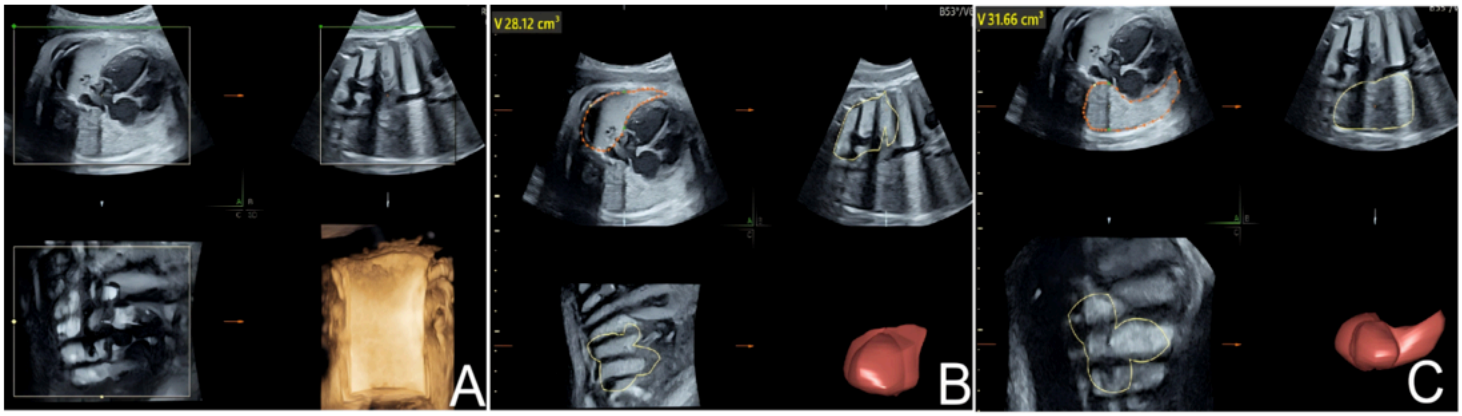


Figure 3

Application of three-dimensional VOCAL technique for measuring fetal lung volume at 34 weeks of gestation in the control group (A-C): (A) Three-dimensional view of the fetal four-chamber transverse view; (B) Left lung volume measured 28.12 cm³; (C) Right lung volume measured 31.66 cm³. (VOCAL:Virtual Organ Computer-aided Analysis; cm³: cubic centimeters)

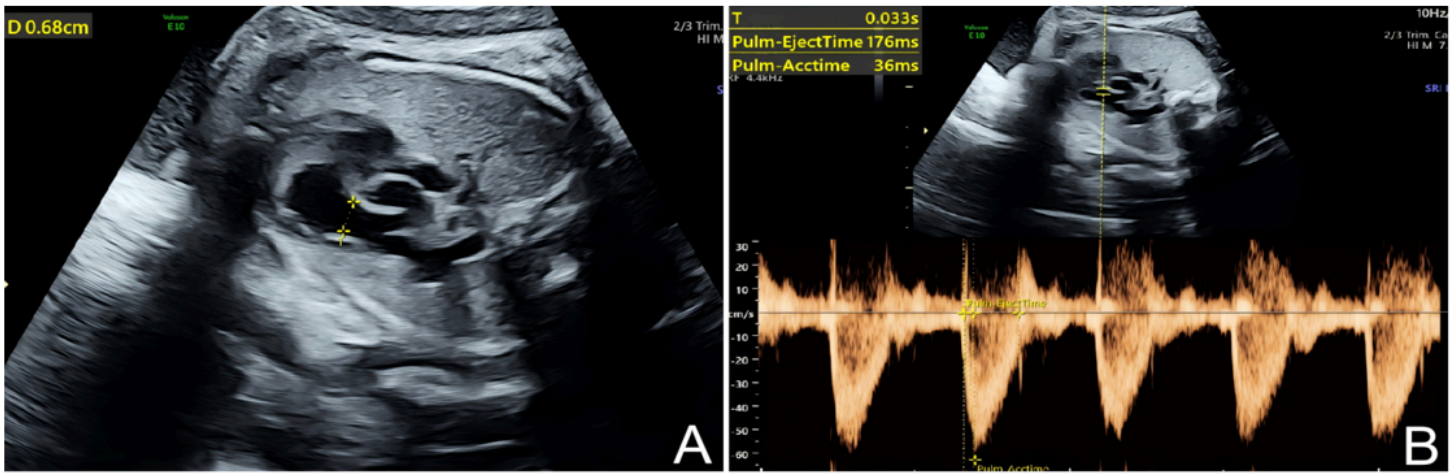


Figure 4

Main pulmonary artery diameter and spectral Doppler ultrasound parameters in a fetus at 39 weeks of gestation from the case group (A-B): (A) The main pulmonary artery diameter measured 6.8 mm at the level of the pulmonary valve tips; (B) AT was 36 ms, and ET was 176 ms.(AT: acceleration time; ET: ejection time; mm: Millimeter; ms: milliseconds)

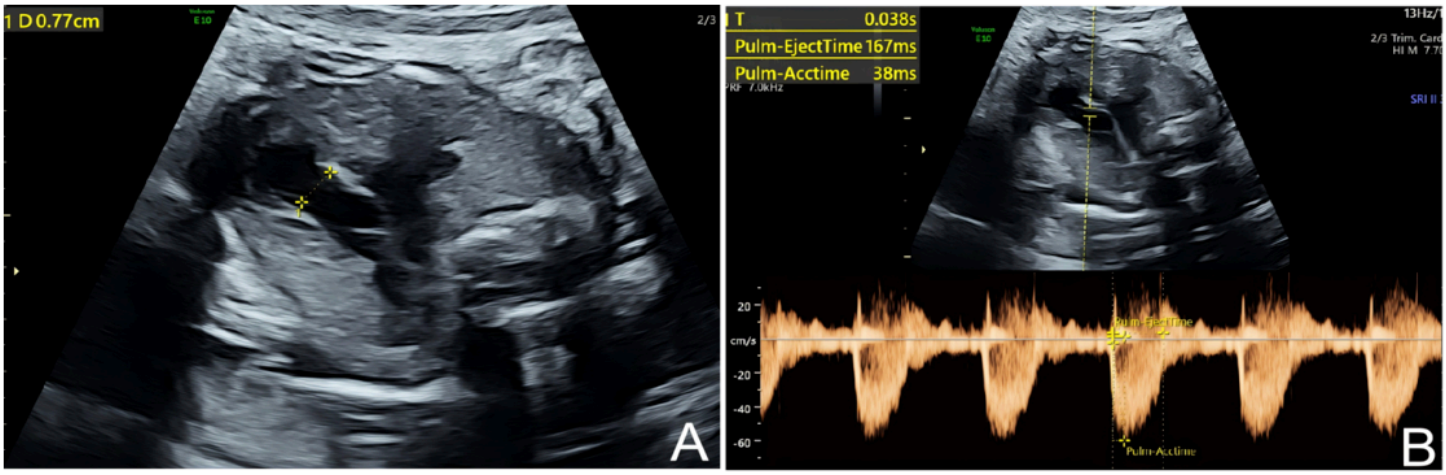


Figure 5

Main pulmonary artery diameter and spectral Doppler ultrasound parameters in a fetus at 39 weeks of gestation from the control group (A-B): (A) The main pulmonary artery diameter measured 7.7 mm at the level of the pulmonary valve tip; (B)AT was 38 ms, and ET was 167 ms.(AT: acceleration time; ET: ejection time; mm: Millimeter; ms: milliseconds)

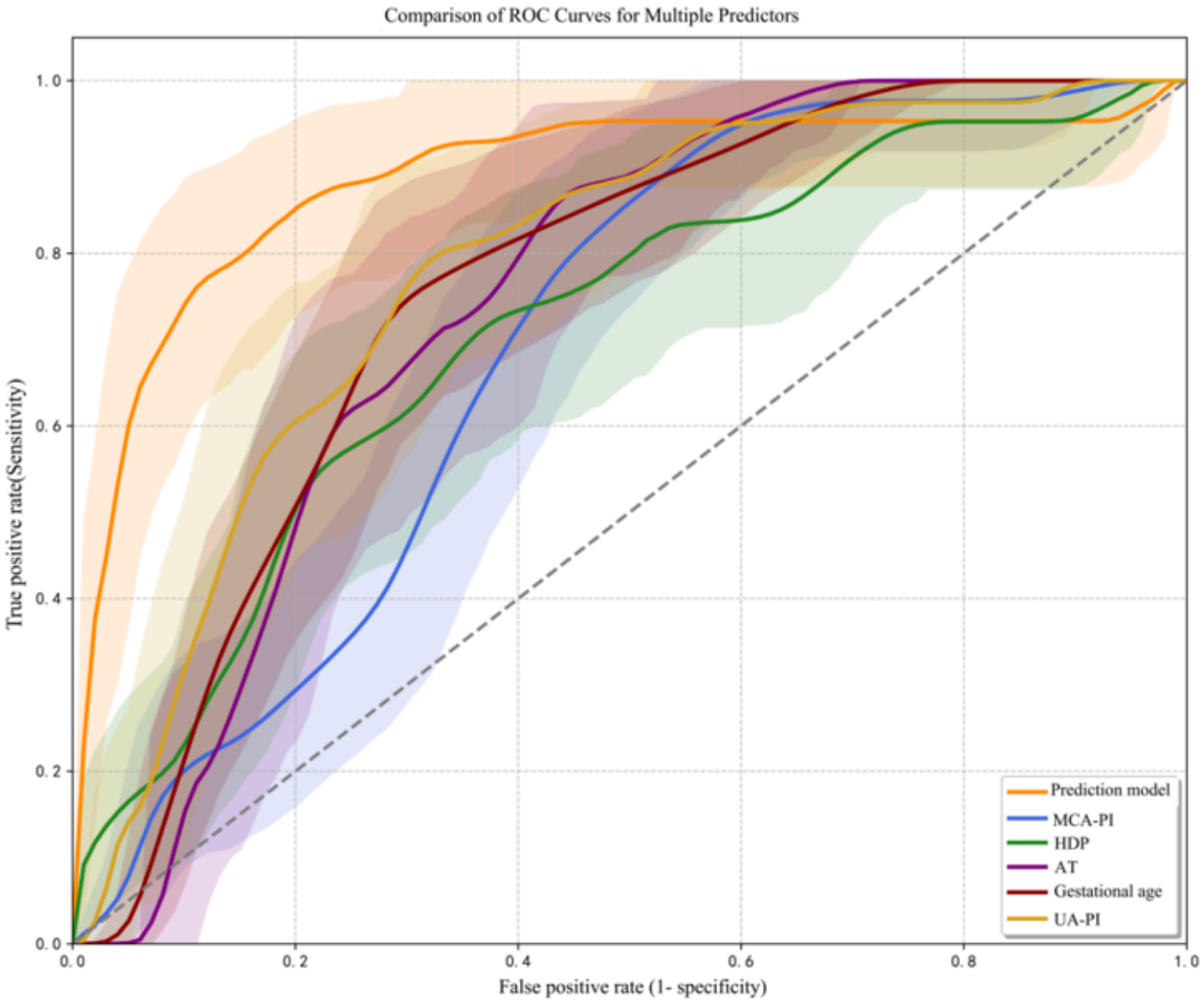


Figure 6

Comparison of ROC curves between the combined prediction model and individual predictors

Supplementary Files

This is a list of supplementary files associated with this preprint. Click to download.

- Tables.pdf